Triple-Helix Formation at Different Positions on Nucleosomal DNA†

Philip M. Brown,‡ Christopher A. Madden, and Keith R. Fox*

Division of Biochemistry and Molecular Biology, School of Biological Sciences, University of Southampton, Bassett Crescent East, Southampton SO16 7PX, United Kingdom

Received July 22, 1998; Revised Manuscript Received September 23, 1998

ABSTRACT: We have prepared a series of seven DNA fragments, based on the 160 base-pair *tyr*T sequence, which contain 12−14 base-pair oligopurine tracts at different positions, and have examined their availability for triple-helix formation after reconstituting onto nucleosome core particles. By using DNase I footprinting we find that in general, triplexes can only be formed at sites located toward the ends of nucleosomal DNA fragments. For the native fragment, bases 1−145 are in contact with the protein surface. Stable triplexes can be formed on these nucleosome-bound fragments for sites located before position 33 and beyond position 94. These are formed with both CT-containing oligonucleotides, generating parallel triplexes at pH 5.5, and GT-containing oligonucleotides forming antiparallel triplexes at pH 7.5. No antiparallel triplexes were formed at sites located between these positions. Parallel triplexes were also not formed at sites between positions 39−50 and 43−54 with oligonucleotide concentrations as high as 30 μM. However parallel triplex formation was evident at a site between positions 48 and 59, albeit with a reduced affinity compared to free DNA, suggesting that this oligopurine tract is less tightly associated with the nucleosome surface or that it has an altered translational position. The introduction of an oligopurine tract in the vicinity of the nucleosome dyad caused the fragment to adopt a different nucleosomal position, which could be targeted with parallel, but not antiparallel triplexes.

The structure of double-helical DNA has been known for over 40 years, and its interaction with various enzymes and structural proteins has been described in detail. However, within the last 15 years it has become apparent that DNA can adopt a range of other structures including left-handed duplexes, triplexes, and quadruplexes, the formation of which depends on conditions such as ionic strength, superhelical stress, and protein binding (*1*). One of these structures, which has received considerable attention is triplex DNA (*2*). This can be generated either by disproportionation of a DNA duplex under superhelical stress, forming an *intra*molecular triplex (*3, 4*), or by addition of an appropriate oligonucleotide to a duplex target, generating an *inter*molecular triplex (*5*−*7*). Polypurine tracts are often located in promoter regions and may have a role in gene regulation (*8, 9*). The formation of DNA triple helixes offers a means of designing compounds which are able to recognize unique DNA sequences, and which may be used as antigene agents or experimental tools (*10*−*13*).

Intermolecular DNA triple helixes are formed when a third oligonucleotide strand binds in the major groove of duplex DNA. The third strand bases form hydrogen bond contacts with substituents on the duplex base pairs, usually interacting with the purine base. It is for this reason that these structures are normally restricted to homopurine·homopyrimidine tracts. Two main types of triplex have been characterized, which differ in the orientation of the third strand. Pyrimidine-rich oligonucleotides bind parallel to the duplex purine strand and form T·AT and C^+·GC triplets (*5, 7*). Conditions of low pH (<5.5) are required to ensure protonation of the third strand cytosines (*14, 15*). In contrast GA- and GT-containing oligonucleotides bind antiparallel to the duplex purine strand, forming G·GC, A·AT, and T·AT triplets (*16*−*18*).

There have been numerous studies examining the formation of intermolecular triplexes in vitro. However cellular DNA is packed into higher order chromatin structures which may alter DNA conformation or mask potential binding sites. The basic unit of chromatin is the nucleosome, which consists of two copies of each of the four histones (H2A, H2B, H3, and H4) around which 146 base pairs of DNA are wrapped 1.65 times forming a left-handed superhelix (*19*−*22*). Although this structure must be able to form on most if not all DNA sequences, there is considerable evidence that DNA fragments adopt preferred rotational and translational settings on the nucleosome surface (*23*−*27*). Although little is known about the factors affecting translational positioning, the rotational position of DNA sequences with respect to the protein surface is known to depend on anisotropic DNA flexibility (*28*). Since DNA must bend as it wraps around the protein core, sequences which facilitate bending have been implicated in directing nucleosome assembly. In general GC-rich regions are positioned with their wider than average minor grooves facing away from the protein core, while the narrow minor grooves of AT sequences face toward the protein (*24, 25*). Certain repetitive sequences, as well

‡ Present address: Department of Haematology, University of Cambridge, EABC, Long Road, Cambridge CB2 2PT, U.K.

† This work was supported by grants from the Medical Research Council, the Cancer Research Campaign and the Association for International Cancer Research.

* Corresponding author: Dr Keith R. Fox, Division of Biochemistry and Molecular Biology, School of Biological Sciences, University of Southampton, Bassett Crescent East, Southampton SO16 7PX, U.K. Telephone: +1703-594374. Fax: +1703-594459. E-mail: KRF1@soton.ac.uk.

10.1021/bi981768n CCC: $15.00
Published on Web 10/30/1998

Table 1: Preparation and Properties of the DNA Fragments Containing Oligopurine Tracks Used in This Work[a]

DNA fragment	mutagenic primer	template	target sequence	parallel	antiparallel
*Tyr*T(22−33)	GGTTGCGTTCTTTTCTTCCGTAACG	*Tyr*T	GGAAGAAAAGAA	CCTTCTTTTCTT	TTGTTTTGTTGG
*Tyr*T(39−50)	GAGAAAAAAGAAGAGGTTGCG	*Tyr*T(43−54)	AAAAAGAAGAGG	TTTTTCTTCTCC	GGTGTTGTTTTT
*Tyr*T(43−54)	GAAAAAAGAACTGG	*Tyr*T	GAGAAAAAAGAA	CTCTTTTTTCTT	TTGTTTTTTGTG
*Tyr*T(48−59)	GTGTTAGGAAGAGAAAA	*Tyr*T(43−54)	AGGAAGAGAAAA	TCCTTCTCTTTT	TTTTGTGTTGGT
*Tyr*T(69−75)	CGAAGGAGAAAAGAGTTACGTT	*Tyr*T			
*Tyr*T(62−75)	ATGACGCGAAGGAGTAAAGT	*Tyr*T(69−75)	GAAGGAGAAAAGAG	CTTCCTCTTTTCTC	GTGTTTTGTGGTTG
*Tyr*T(94−106)	CGGGAAGAGGGGAGCATCAT	*Tyr*T	GGGAAGAGGGGAG	CCCTTCTCCCCTC	GTGGGGTGTTGGG
*Tyr*T(107−120)	GGCCTTCTCCCTTCTCGGAA	*Tyr*T	GAGAAGGGAGAAGG	CTCTTCCCTCTTCC	GGTTGTGGGTTGTG

[a] Parallel and antiparallel refer to the sequence of the triplex-forming oligonucleotides used to form parallel and antiparallel triplexes.

as double-stranded RNA will not wrap around nucleosomes (*29*), although recent studies have shown that long blocks of $A_n \cdot T_n$ may not be excluded (*30, 31*). Within each DNA fragment it is not possible to satisfy all the local preferences; sequences at the center of a nucleosome have a greater effect on rotational positioning than those toward the ends (*32*). Solution studies on reconstituted nucleosomes suggested that the helical repeat of DNA varies along the nucleosome from 10.0 base pairs per turn at the ends to 10.7 at the dyad, compared with a value of 10.5 for DNA free in solution (*27*). The crystal structure of the nucleosome core particle at 2.8 Å resolution also shows that the double-helical parameters vary over the length of the superhelix between 9.4 and 10.9 base pairs per turn (*22*). In addition the histone core exerts a dominant effect on DNA structure so that sequences which form different structures in free solution adopt similar conformations when bound to the nucleosome (*33, 34*).

The interaction of DNA with nucleosome core particles may present a problem for triplex formation, since the third strand oligonucleotide must wrap around the DNA duplex which is already wrapped around the protein core. If the third strand spans more than 10 base pairs it will have to thread between the protein surface and the duplex in order continually to access the DNA major groove. Previous work has shown that triplex formation alters nucleosomal arrangement and functions as a nucleosomal barrier (*35, 36*), placing the triple-helical regions on the internucleosomal DNA. We have also shown that DNA which has been assembled onto nucleosomes is not available for triplex formation, though target sites toward the ends of nucleosomal fragments, in regions where the DNA is less tightly associated with the protein core can still be targeted (*37*). In this paper we have prepared a series of DNA fragments possessing oligopurine target sites at different positions, and have examined their availability for triplex formation after reconstituting onto nucleosome core particles. For these studies we have used the *tyr*T DNA fragment, since its interaction with nucleosome core particles has been well-documented (*25*).

MATERIALS AND METHODS

Chemicals and Enzymes. Oligonucleotides for triplex formation, PCR, and site directed mutagenesis were purchased from Oswel DNA service. These were stored in water at −20 °C, and diluted to working concentrations immediately before use. Plasmid pUC18 was purchased from Pharmacia. DNase I was purchased from Sigma and stored at −20 °C at a concentration of 7200 U/mL. Restriction enzymes and reverse transcriptase were purchased from Promega. The triplex-binding naphthylquinoline derivative (*38*−*40*) was a gift from Dr. L. Strekowski, Department of Chemistry, Georgia State University. This was stored as a 20 mM stock solution in dimethyl sulfoxide at −20 °C, and diluted to working concentrations immediately before use.

DNA Fragments. The *tyr*T DNA fragment was used for these studies since it has been widely studied and its interaction with nucleosome core particles has been fully characterized, revealing that the first 145 base pairs are closely associated with the protein (*25*). Oligopurine tracts of 12−14 base pairs in length were introduced into this fragment by PCR-mediated site-directed mutagenesis, using the mutant primers and DNA templates indicated in Table 1. The resulting fragments were cloned between the *Eco*R1 and *Ava*1 sites of pUC18. In general the modifications were chosen so as to introduce conservative changes to the DNA sequence (replacing TA with AT and CG with GC) and were placed in regions which required only two or three base changes. However introduction of an oligopurine tract into the center of the fragment, around the nucleosome dyad, required six bases changes and was prepared by first generating *tyr*T(69−75) before a second round of PCR-mediated mutagenesis generating *tyr*T(62−75). The sequences of the resulting fragments, which are shown in Figure 1 were confirmed by DNA sequencing using a T7 sequencing kit (Pharmacia). Radiolabeled DNA fragments were prepared by digesting the plasmids with *Eco*R1 and *Sma*1 and were labeled at the 3′-end of the *Eco*R1 site with α-[^{32}P]dATP using reverse transcriptase. Radiolabeled DNA was separated from the remainder of the plasmid on 6% nondenaturing polyacrylamide gels. The bands containing the radiolabeled DNA were excised and eluted into 10 mM Tris-HCl pH 7.5 containing 0.1 mM EDTA. The DNA was then precipitated with ethanol in the presence of 0.3 M sodium acetate.

Reconstitution of DNA onto Nucleosome Core Particles. H1-stripped chromatin, derived from chicken erythrocytes, was prepared as previously described (*24, 25*) and stored at 4 °C, or −20 °C in 50% (v/v) glycerol. The DNA fragments of interest were reconstituted onto nucleosomes at pH 7.5 by a salt exchange method, as previously described (*23*−*25*). Radiolabeled DNA (∼1 nmol base pairs) was dissolved in 12 μL of 20 mM Tris-HCl pH 7.4 containing 1 mM EDTA. This was mixed with 18 μL of nucleosome core particles (12 mg/mL) and 8 μL of a high salt buffer containing 30 mM Tris-HCl pH 8.0, 4.5 M NaCl, and 5 mM EDTA. This was incubated at 37 °C for 30 min before slowly decreasing the salt concentration to 100 mM by stepwise additions of 5 mM Tris-HCl pH 8.0 containing 1 mM EDTA, and 0.1% (v/v) Nonidet P40. The incorporation of labeled DNA onto nucleosomes was checked by gel

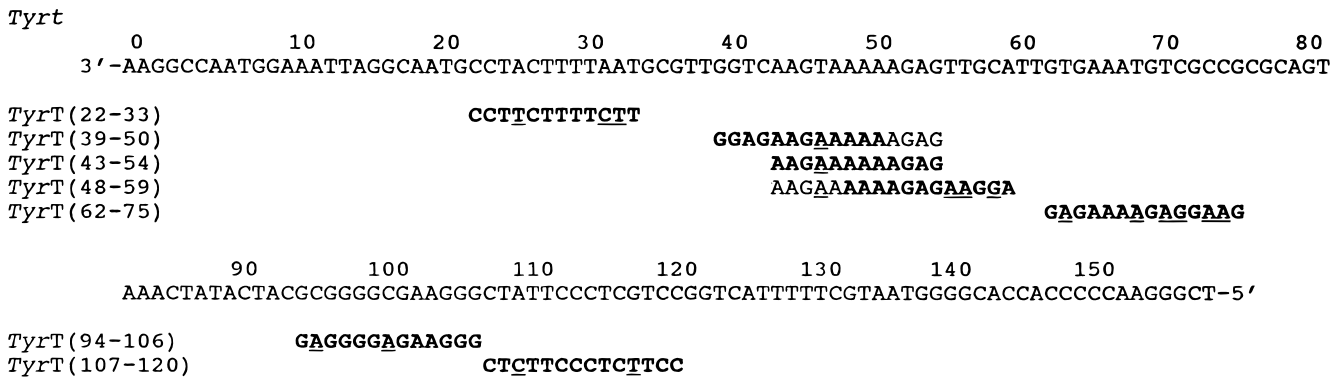

FIGURE 1: Sequences of the *tyr*T mutants used in this study. The full sequence (which is written from 3′ to 5′) shows the original *tyr*T fragment. The numbering scheme corresponds to that used in previous studies with *tyr*T DNA (*44*). The individual oligopurine tracts in each mutant are shown below the original sequence, in which base changes are underlined. Only the portions of each tract which are shown in bold were targeted with triplex forming oligonucleotides.

retardation on 1% (w/v) agarose gels; at least 95% of the labeled DNA was included in the retarded species. These reconstituted nucleosomes were stored at 4 °C.

Footprinting Reconstituted Core Particles. A total of 10 μL of the reconstituted nucleosomes was mixed with 10 μL of varying concentrations of oligonucleotides dissolved in either 50 mM sodium acetate pH 5.5 containing 10 mM $MgCl_2$ and 50 mM NaCl (for parallel triplexes) or 10 mM Tris-HCl pH 7.5 containing 100 mM NaCl and 10 mM $MgCl_2$ (for antiparallel triplexes). Where indicated some experiments with antiparallel triplexes used 10 mM $MnCl_2$ instead of 10 mM $MgCl_2$, as we find that this divalent metal ion increases the stability of antiparallel triplexes. In some instances, especially with antiparallel triplexes 10 μM of a naphthylquinoline triplex-binding ligand was included in the incubation in order to enhance triplex stability. These mixtures were allowed to equilibrate for at least 1 h before digesting with either DNase I or a hydroxyl radical generating mixture. DNase I digestion was achieved by adding 4 μL of enzyme (typically 30 U/mL) dissolved in 20 mM NaCl, 2 mM $MgCl_2$, 2 mM $MnCl_2$. Higher concentrations of DNase I are required for digesting the nucleosome bound DNA fragments than for free DNA due to the presence of the large amount of unlabeled DNA from the chicken nucleosomes; the enzyme concentration was adjusted so that about 60−70% of the DNA remained uncut. The digestion was stopped after 1 min by the addition of 100 μL of phenol. Hydroxyl radical cleavage was performed by adding 40 μL of a freshly prepared mixture containing 50 μM ferrous ammonium sulfate, 100 μM EDTA, 2 mM ascorbic acid, and 0.05% hydrogen peroxide. The reaction was stopped after 8 min by adding 100 μL of phenol and the aqueous phase was made up to 100 μL with water. The samples were then extracted twice with phenol, to remove the protein, followed by two extractions with ether to remove the remaining phenol. The DNA was finally precipitated with ethanol and redissolved in 8 μL of 80% formamide containing 10 mM EDTA, 10 mM NaOH, and 0.1% (w/v) bromophenol blue.

Footprinting Free DNA. Radiolabeled DNA was dissolved in 10 mM Tris-HCl pH 7.5 containing 0.1 mM EDTA. A total of 1.5 μL of this DNA solution was mixed with 3 μL of oligonucleotide, dissolved 10 mM Tris-HCl pH7.5 containing 100 mM NaCl and 10 mM $MgCl_2$ (for antiparallel triplexes) or 50 mM sodium acetate pH 5.5 containing 10 mM $MgCl_2$ and 50 mM NaCl (for parallel triplexes). This mixture was allowed to equilibrate for at least 1 h before digesting with either DNase I or a hydroxyl radical generating mixture. DNase I digestion was achieved by adding 2 μL of enzyme (typically 0.01 U/mL) dissolved in 20 mM NaCl, 2 mM $MgCl_2$, 2 mM $MnCl_2$. The digestion was stopped after 1 min by adding 5 μL of 80% formamide containing 10 mM EDTA, 10 mM NaOH, and 0.1% (w/v) bromophenol blue. Hydroxyl radical cleavage was performed by adding 6 μL of a freshly prepared mixture containing 50 μM ferrous ammonium sulfate, 100 μM EDTA, 2 mM ascorbic acid, and 0.05% hydrogen peroxide. The reaction was stopped after 8 min by precipitating with ethanol. The DNA was finally redissolved in 8 μL of 80% formamide containing 10 mM EDTA, 10 mM NaOH, and 0.1% (w/v) bromophenol blue.

Gel Electrophoresis. Products of digestion were separated on 6−10% polyacrylamide gels (depending on the location of the target site) containing 8 M urea. DNA samples were boiled for 3 min immediately before loading onto the gels. Polyacrylamide gels (40 cm long) were run at 1500 V for 2 h. These were then fixed in 10% acetic acid, transferred to Whatmann 3MM paper, dried under vacuum at 80 °C, and exposed to autoradiography at −70 °C with an intensifying screen. The products of digestion were assigned by comparison with Maxam−Gilbert marker lanes specific for guanine and adenine. Autoradiographs of hydroxyl radical cleavage were scanned using a Hoefer 365W microdensitometer.

RESULTS

We have previously shown that triplex formation at a 12 base-pair oligopurine tract between positions 43 and 54 on a modified *tyr*T DNA fragment can be blocked by association of the DNA with nucleosome core particles (*37*). In the present studies we systematically examine the formation of similar triplexes at oligopurine tracts which have been placed at different positions along the *tyr*T DNA fragment. The sequences of these fragments are shown in Figure 1, while the third strand oligonucleotides, designed for either parallel or antiparallel triplex formation, are presented in Table 1.

A potential problem with altering the DNA sequence is that since the rotational and translational position of DNA on the nucleosome is indirectly determined by the DNA

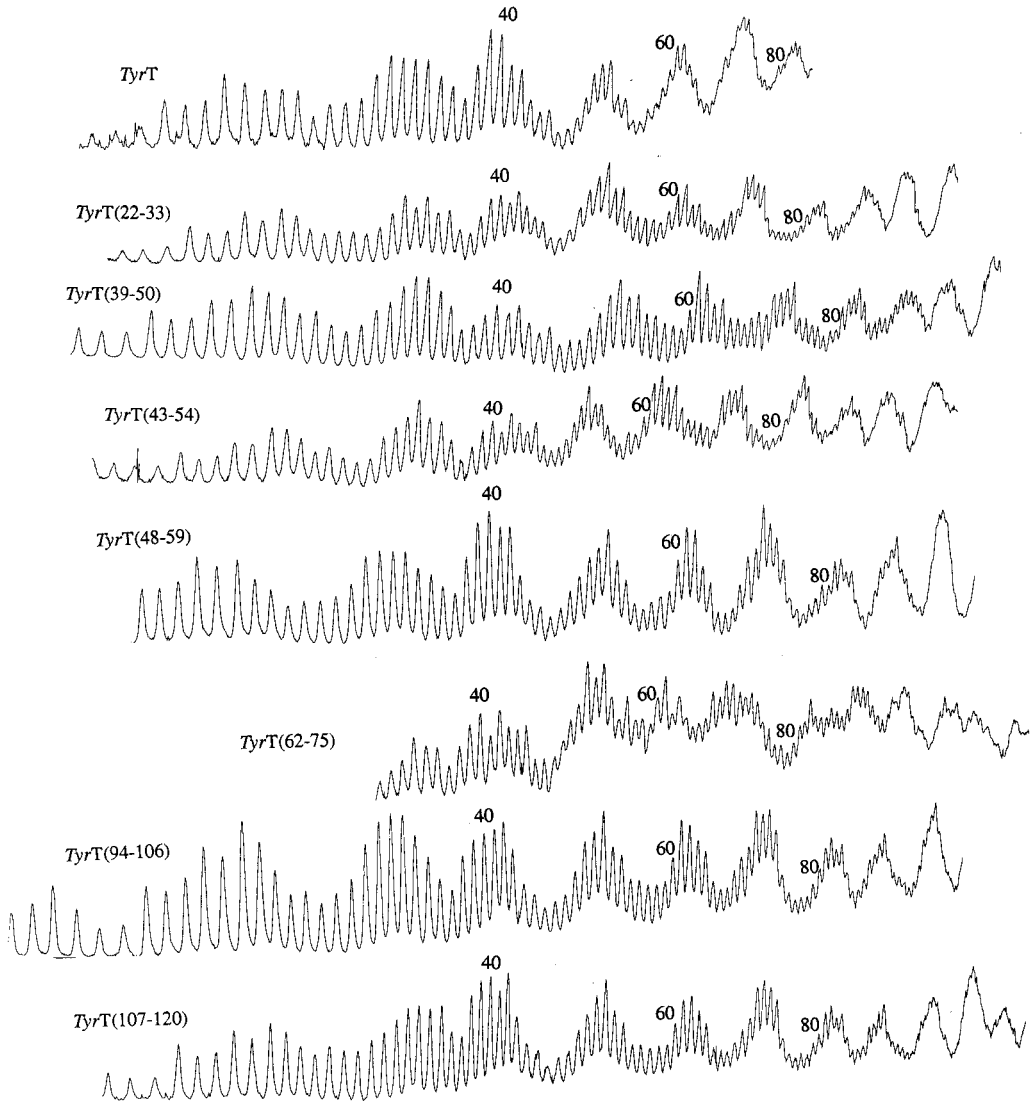

FIGURE 2: Densitometer traces of hydroxyl radical cleavage for each of the mutant *tyr*T DNA when complexed with nucleosome core particles.

sequence, these changes might alter its position relative to that of the native fragment. This would complicate any comparison of triplex formation at the different locations. This may be especially relevant for oligopurine tracts since polydA·polydT does not easily wrap around nucleosomes. However, it should be noted that $(GA)_n$·$(TC)_n$ tracts have been found within chicken erythrocyte DNA and show no preferential rotational or translational orientation (*41*). Similarly other $(GA)_n$·$(TC)_n$ tracts have been shown to form nucleosomes in vitro (*35*, *42*, *43*). The rotational position of these mutated *tyr*T fragments when reconstituted onto nucleosome core particles was therefore checked by examining their hydroxyl radical cleavage patterns. Densitometer traces of these nucleosome-bound cleavage patterns are shown in Figure 2. In each case it can be seen that, as expected, these reconstituted fragments generate a sinusoidal cleavage pattern with a 10-base repeat, in contrast to free DNA (not shown) which produces a fairly even cleavage pattern. With the exception of *tyr*T(62−75), there are only minor differences between the various cleavage patterns with maximal cleavage evident around positions 21−23, 32−33, 40−42, 51−53, 61−62, 71−74, 83−85, 92−95, and 103−105. We therefore conclude that these fragments adopt very similar rotational positions, although, as discussed later we cannot be sure of their translational locations. However the pattern for *tyr*T(62−75), in which the oligopurine tract is located close to the original nucleosomal dyad, is significantly different. Although hydroxyl radical cleavage of this reconstituted fragment is not even, the simple 10-base repeat is no longer evident. Some of the strongest peaks seen with the other fragments are still evident, but these are accompanied by additional peaks around positions 34−35, 43−45, 54−55, 76−78, and 86−90. These indicate that this DNA fragment is not sitting in the same position on the nucleosome cores and suggest that it does not adopt a unique rotational setting. This will be considered further in the section examining triplex formation at this target site.

The translational position of each fragment is much less well-defined. For the native *tyr*T DNA fragment positions 0−145 are thought to interact with the protein surface. This might be altered for any of these mutated fragments, and could be further affected on interaction with the triplex-forming oligonucleotides. However, we failed to detect any change in micrococcal nuclease digestion of the various fragments when assembled onto nucleosome core particles (not shown). In addition examination of Figure 1 shows at

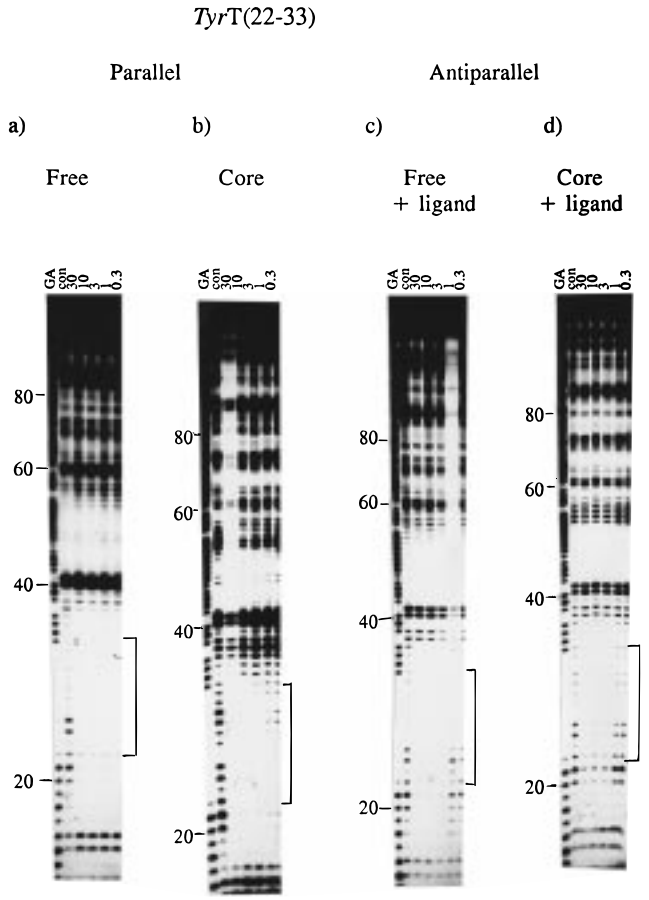

FIGURE 3: DNase I cleavage patterns of *tyr*T(22−33) in the presence and absence of parallel and antiparallel oligonucleotides when free or complexed with nucleosome core particles. The position of the triplex target site is indicated by the square brackets. "con" indicates cleavage of the DNA in the absence of oligonucleotide. Oligonucleotide concentrations (μM) are indicated at the top of each gel lane. Tracks labeled "GA" are Maxam−Gilbert sequencing lanes specific for purines. Panels a and b show the results of parallel triplex formation and were performed in 50 mM sodium acetate pH 5.5 containing 50 mM NaCl and 10 mM $MgCl_2$. Panels c and d show antiparallel triplex formation and were performed in 10 mM Tris-HCl pH 7.5 containing 10 mM $MgCl_2$ and 100 mM NaCl in the presence of 10 μM naphthylquinoline triplex-binding ligand.

least eight peaks in each of the phased hydroxyl radical cleavage patterns, suggesting that the region between positions 20−110 is associated with the protein surface in every case.

For each fragment described below the integrity of the reconstituted nucleosome was checked both before and after addition of the triplex-forming oligonucleotides by agarose gel electrophoresis. In each case at least 95% of the radiolabeled DNA was associated with the retarded species.

TyrT(22−33). This sequence contains a 12 base-pair oligopurine triplex target site (GGAAGAAAAGAA) between bases 22 and 33 [the numbering system is taken from the original *tyr*T sequence (*44, 45*)]. We have targeted this with the parallel triplex forming oligonucleotide CCTTCTTTTCTT generating 8×T·AT and 4×C^+·GC triplets or the antiparallel triplex forming oligonucleotide TTGTTTTGTTGG generating 8×T·AT and 4×G·GC triplets. The results of DNase I footprinting experiments with free and core-bound DNA are presented in Figure 3.

Panel a shows DNase I digestion of free DNA in the presence and absence of the parallel triplex-forming oligonucleotide. Although DNase I cleavage of this and other target sites is not good since oliogopurine sequences (especially A_n·T_n) are poor substrates for this enzyme, a clear oligonucleotide-induced footprint can be seen which is most clearly evident from protection of the bands at positions 20−25. This footprint persists to the lowest oligonucleotide concentration presented (0.3 μM). All the experiments with parallel triplex-forming oligonucleotides described in this paper were performed at pH 5.5, necessary for forming the C^+·GC triplet. We find that although there are subtle changes between the DNase I cleavage patterns at these two pHs (compare the control lanes of panels b and d), this low pH does not affect nucleosome integrity, as previously reported (*37*). Panel b of this Figure shows the results of a similar experiment in which the DNA is now associated with nucleosome core particles. As expected, the cleavage pattern changes on association with the protein core; in particular, new cleavage products are evident around positions 30, 46/47, and 52−55. It can be seen that the oligonucleotide still produces a footprint at this site when the DNA is complexed to the nucleosome cores. Parallel triplex formation at this site therefore appears not to be hindered by wrapping the DNA fragment around the nucleosome cores, and contrasts with our previous results with *tyr*T(43−54) (*37*). We can exclude the possibility that this footprint (and others described below) is caused by interaction of the oligonucleotide with a small amount of contaminating free DNA since we have shown that in every instance at least 95% of the DNA is associated with the nucleosome cores, even after adding the triplex-forming oligonucleotide.

Panels c and d show the results of similar experiments with the GT-containing oligonucleotide which has been designed to form an antiparallel triplex. These experiments were performed at pH 7.5 in the presence of 10 mM $MgCl_2$. With both free and core-bound DNA, no footprints are observed with the oligonucleotide alone (not shown), presumably because this short triplex, which consists of mainly T·AT triplets, is not sufficiently stable. However on addition of 10 μM naphthylquinoline triplex-binding ligand (*38−40*), a clear footprint is evident at the target site with oligonucleotide concentrations of 3 μM and above. This footprint is evident with both free and core-bound DNA, although close inspection of the patterns for core-bound DNA reveals that some attenuated cleavage products are still evident within the lower part of the target site, around positions 20−22. Since these are fully protected with the free DNA it seems that the nucleosome cores have altered the accessibility of this part of the target site and have hindered the interaction with this end of the target sequence.

These results with *tyr*T(22−33), demonstrating the possibility of forming triplexes on nucleosome-bound DNA fragments, are at variance with our previous studies with *tyr*T(43−54) for which triplex formation was prevented. It seems reasonable to suppose that this difference arises from the location of the triplex target sites relative to the ends of the fragment, although it could also be due to their different rotational position relative to the nucleosome surface. We therefore generated further DNA fragments containing triplex-binding sites at different positions.

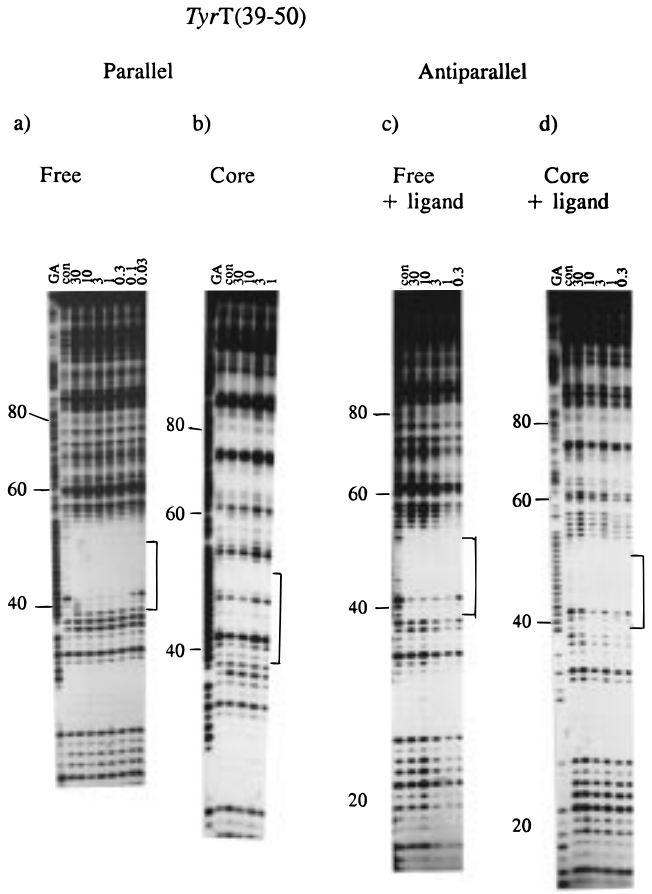

FIGURE 4: DNase I cleavage patterns of *tyr*T(39−50) in the presence and absence of parallel and antiparallel oligonucleotides when free or complexed with nucleosome core particles. The position of the triplex target site is indicated by the square brackets. "con" indicates cleavage of the DNA in the absence of oligonucleotide. Oligonucleotide concentrations (μM) are indicated at the top of each gel lane. Tracks labeled "GA" are Maxam−Gilbert sequencing lanes specific for purines. Panels a and b show the results of parallel triplex formation and were performed in 50 mM sodium acetate pH 5.5 containing 50 mM NaCl and 10 mM $MgCl_2$. Panels c and d show antiparallel triplex formation and were performed in 10 mM Tris-HCl pH 7.5 containing 10 mM $MnCl_2$ and 100 mM NaCl in the presence of 10 μM naphthylquinoline triplex-binding ligand.

*TyrT(*39−50). This DNA fragment contains a 12 base-pair oligopurine triplex target site (AAAAAGAAGAGG), which is 17 base pairs removed from the target site in *tyr*T-(22−33), approximately 1.5 helical turns toward the center of the DNA fragment. This can be targeted by the parallel triplex forming oligonucleotide TTTTTCTTCTCC generating 8×T·AT and 4×C^+·GC triplets or the antiparallel triplex forming oligonucleotide GGTGTTGTTTTT generating 8×T·AT and 4×G·GC triplets. The results of DNase I footprinting experiments with this free and core-bound DNA are presented in Figure 4.

Panels a and b show the interaction of the parallel triplex-forming oligonucleotide with free and core bound *tyr*T(39−50). Panel a reveals a footprint with the free DNA which is most clearly evident from the protection at the top (50) and bottom (41) of the target site, which persists to an oligonucleotide concentration of 0.3 μM. This footprint is accompanied by enhanced cleavage at the triplex−duplex junction (position 39). Such enhanced cleavage has previously been observed with other triplexes and is generally found on the duplex purine strand at the triplex−duplex junction (*39, 46*). When this fragment is associated with nucleosome core particles (panel b) no footprints are observed, even at an oligonucleotide concentration as high as 30 μM. Binding was not induced by addition of 10 μM triplex-binding ligand (not shown).

A similar result is seen for antiparallel triplex formation at this target site (panels c and d). As seen with *tyr*T(22−33) footprints are only observed with free DNA after addition of 10 μM triplex-binding ligand. In the presence of this ligand an oligonucleotide-induced footprint is evident which persists to an oligonucleotide concentration of 0.3 μM; this is most clearly evident from the bands at the edges of the target site at positions 41 and 51. On placing this fragment onto nucleosome cores, no antiparallel triplex formation is seen (panel d), even in the presence of the triplex-binding ligand.

These results show that moving the target site 17 bases along the sequence, toward the center of the core-bound DNA, has abolished both parallel and antiparallel triplex formation. This suggests that the location of the target site relative to the nucleosome core is important for triplex formation.

TyrT(43−54). This fragments contains a 12-base oligopurine tract (GAGAAAAAAGAA) which is located a further 4 bases toward the center of the nucleosome. This will alter the rotational orientation of the triplex site relative to the protein surface by about half a helical turn, so that regions that were facing toward the core in *tyr*T(39−50) will now be turned to face the solution, and vice versa. This site can be targeted with CTCTTTTTTCTT, generating a parallel triplex containing 9×T·AT and 3×C^+·GC triplets, or TTGTTTTTTGTG forming an antiparallel triplex containing 9×T·AT and 3×G·GC triplets. Results with this DNA sequence [previously designated *tyr*T(46A)] have already been presented (*37*) and show that while clear footprints can be formed on this target site with free DNA, this is inhibited by interaction with the nucleosome.

TyrT(48−59). This DNA fragment contains a twelve base oligopurine tract (AGGAAGAGAAAA) which is located a further 5 bases (half a helical turn) toward the center of the nucleosome. This can be targeted with TCCTTCTCTTTT generating a parallel triplex containing 8×T·AT and 4×C^+·GC triplets or TTTTGTGTTGGT forming an antiparallel triplex containing 8×T·AT and 4×G·GC triplets. The results with this fragment are presented in Figure 5. Panel a shows DNase I digestion of free DNA in the presence of the parallel triplex forming oligonucleotide and reveals a clear footprint at the expected target site, which persist to the lowest concentration presented (0.3 μM). Panel b shows the results of similar experiments when this DNA fragment is reconstituted onto nucleosome core particles. Contrary to expectation a footprint can be seen at this nucleosome-bound target site with the highest oligonucleotide concentration (30 μM); this is most clearly seen by the reduction of the band at position 53. On adding 10 μM triplex binding ligand (panel c) oligonucleotide binding is improved and the footprint persists to a concentration of about 1 μM. It therefore appears that wrapping this fragment around the nucleosome cores has attenuated, but not prevented parallel triplex formation. However close examination of the cleavage patterns in panels b and c reveal that as well as producing

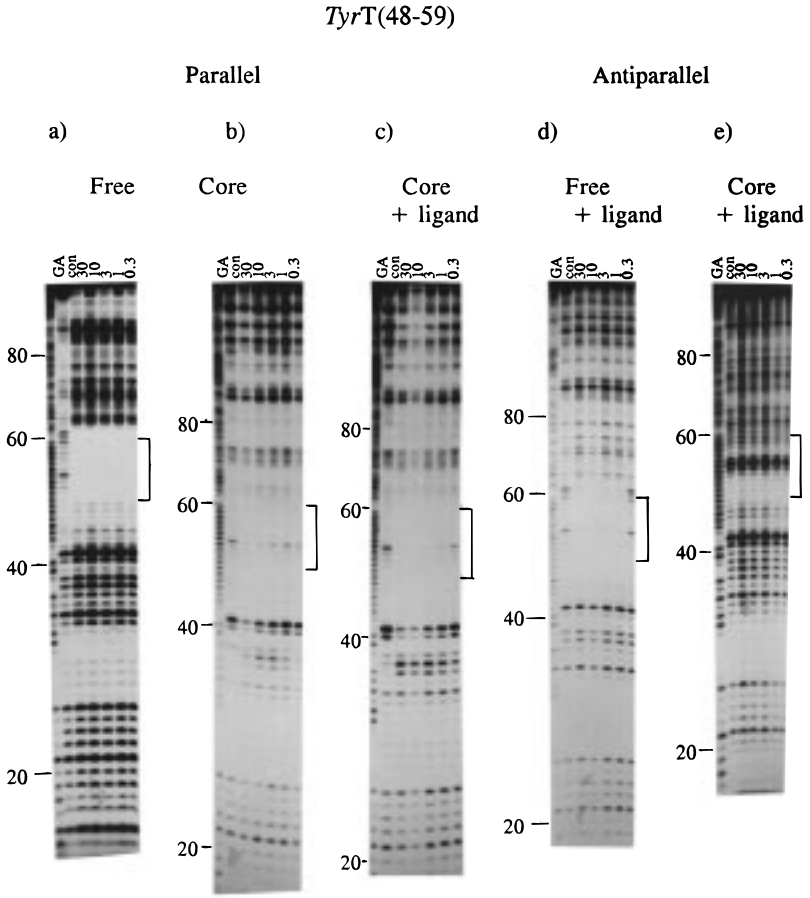

FIGURE 5: DNase I cleavage patterns of *tyr*T(48−59) in the presence and absence of parallel and antiparallel oligonucleotides when free or complexed with nucleosome core particles. The position of the triplex target site is indicated by the square brackets. "con" indicates cleavage of the DNA in the absence of oligonucleotide. Oligonucleotide concentrations (μM) are indicated at the top of each gel lane. Tracks labeled "GA" are Maxam−Gilbert sequencing lanes specific for purines. Panels a and b show the results of parallel triplex formation and were performed in 50 mM sodium acetate pH 5.5 containing 50 mM NaCl and 10 mM $MgCl_2$. Panels c and d show antiparallel triplex formation and were performed in 10 mM Tris-HCl pH 7.5 containing 10 mM $MgCl_2$ and 100 mM NaCl in the presence of 10 μM naphthylquinoline triplex-binding ligand.

a footprint the oligonucleotide has altered the cleavage pattern in the regions immediately below (3′) the target site between positions 33−41. This may indicate a change in nucleosomal conformation and will be considered further in the Discussion.

As with most of the other 12-mer oligonucleotides antiparallel triplex formation at this site was unsuccessful in the absence of added ligand. However, on addition of 10 μM triplex-binding ligand (Figure 5, panel d) a footprint is evident which persists to an oligonucleotide concentration of 1 μM. When this fragment is wrapped around the nucleosome cores (panel e) no triplex footprint is produced. The different interaction of this nucleosome-bound DNA fragment with parallel and antiparallel triplex-forming oligonucleotides could be caused by differences in their strength of binding, since the short parallel triplexes are clearly more stable than their antiparallel counterparts. This will be considered further in the Discussion.

TyrT(62−75). This fragment, which contains a 14-base oligopurine sequence GAAGGAGAAAAGAG, can be targeted by CTTCCTCTTTTCTC generating a parallel triplex containing 8×T·AT and 6×C^+·GC triplets or GTGTTTTGTGGTTG forming an antiparallel triplex containing 8×T·AT and 6×G·GC triplets. Although this fragment was generated in order to examine triplex formation in the vicinity of the nucleosome dyad, it should be remembered that the hydroxyl radical cleavage plots, presented in Figure 2, suggest that it no longer adopts a unique rotational setting. Examination of the control DNase I cleavage patterns for free and core-bound DNA (Figure 6) further suggests that the position of this fragment on the nucleosome has altered. In contrast to the other fragments used in this work the DNase I cleavage patterns for free and core-bound DNA are very similar up to position 56, suggesting this region is either loosely bound to the protein or is free in solution, hanging over the end of the core particle. In contrast, above position 56 the patterns for free and core-bound DNA are distinctly different; in particular bands at position 57, 68, and 77 are much stronger in the free than the core-bound DNA, while core-specific cleavage pattern is evident around positions 71/72.

Figure 6 panel a shows parallel triplex formation on free *tyr*T(62−75) and reveals a clear footprint at the expected target site which persist to an oligonucleotide concentration of 1 μM. A strong enhancement can also be seen at the lower (3′) end of this region. Panel b shows the interaction of this oligonucleotide with the core-bound fragment. Contrary to our expectations a clear footprint can be seen on this core-bound DNA which persists to relatively low concentrations (1 μM). This footprint covers the same region

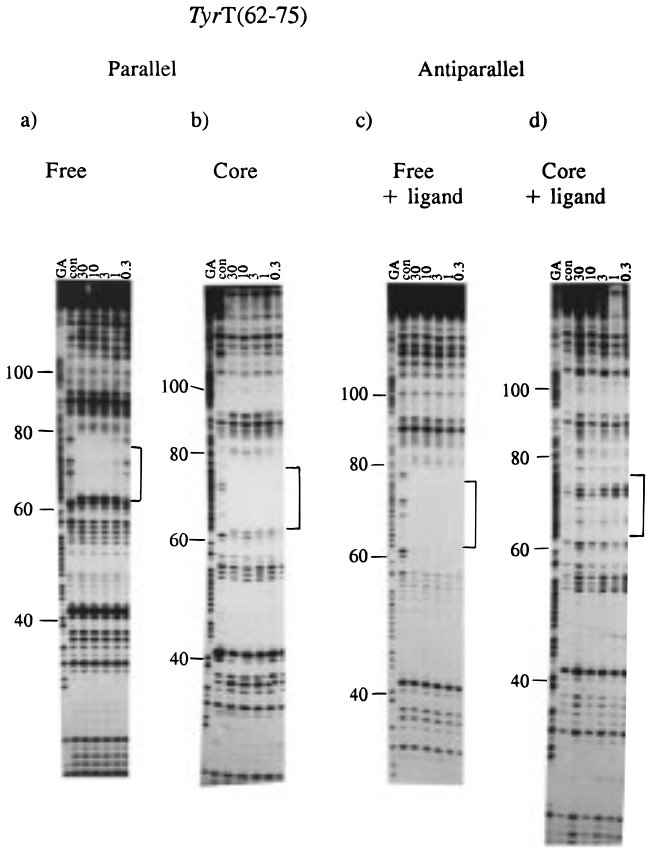

FIGURE 6: DNase I cleavage patterns of *tyr*T(62−75) in the presence and absence of parallel and antiparallel oligonucleotides when free or complexed with nucleosome core particles. The position of the triplex target site is indicated by the square brackets. "con" indicates cleavage of the DNA in the absence of oligonucleotide. Oligonucleotide concentrations (μM) are indicated at the top of each gel lane. Tracks labeled "GA" are Maxam−Gilbert sequencing lanes specific for purines. Panels a and b show the results of parallel triplex formation and were performed in 50 mM sodium acetate pH 5.5 containing 50 mM NaCl and 10 mM $MgCl_2$. Panels c and d show antiparallel triplex formation and were performed in 10 mM Tris-HCl pH 7.5 containing 10 mM $MgCl_2$ and 100 mM NaCl in the presence of 10 μM naphthylquinoline triplex-binding ligand.

as seen with free DNA and is also accompanied by enhanced DNase I cleavage at the 3′ (lower) end. Although the successful formation of a triplex at this site was surprising it is consistent with the suggestion that the nucleosome is bound in a different position relative to the native *tyr*T fragment. If the fragment has moved on the nucleosome it is conceivable that the target site is now located closer to the edge of the nucleosome.

Once again no triplex formation is observed with the GT-containing oligonucleotide in the absence of the triplex-binding ligand, though addition of 10 μM naphthylquinoline triplex-binding ligand induces a footprint which persists to the lowest oligonucleotide concentration (Figure 6, panel c). In contrast to the results with the parallel triplex no footprints are seen with the antiparallel oligonucleotide on the core-bound DNA. This difference will be considered further in the Discussion.

TyrT(94−106). The oligopurine target site was again moved along the original *tyr*T sequence to between bases 94 and 106. This sequence contains the 13 base target site GGGAAGAGGGGAG which can be targeted with the parallel triplex forming oligonucleotide CCCTTCTCCCCTC generating 4×T·AT and 9×C^+·GC triplets and the antiparallel oligonucleotide GTGGGGTGTTGGG, generating 4×T·AT and 9×G·GC triplets. The results are presented in Figure 7. Panel a shows the interaction of the CT-containing parallel oligonucleotide which produces a clear footprint, as expected, which persists to an oligonucleotide concentration of 1 μM, which is accompanied by enhanced DNase I cleavage at the lower (3′) end at the triplex−duplex junction. It should be noted that this triplex contains a higher proportion of C^+·GC triplets than those formed on the other fragments, and may therefore have a higher affinity (*47*). A footprint can also be seen for the interaction of this oligonucleotide with core-bound DNA (panel b) which is evident at the higher oligonucleotide concentrations (10 μM and above), and which is also accompanied by enhanced DNase I cleavage at the 3′ (lower) end. Evidently the nucleosome core is inhibiting triplex formation as a 10-fold higher oligonucleotide concentration is required to produce a footprint on core-bound DNA compared with free. However, in this case it can be seen that the oligonucleotide has affected DNase I cleavage of the region above the target site, which now more closely resembles that in the free DNA. It therefore appears that binding of the oligonucleotide to this target site may have moved the upper regions of the DNA away from the core surface.

Results for antiparallel triplex formation at this site are presented in panels c and d of Figure 7. In contrast to the other antiparallel triplexes described in this paper the GT-containing third strand forms a stable complex at this target site in the absence of the naphthylquinoline triplex-binding ligand. The higher stability of this triplex presumably arises from the greater number of G·GC triplets. With free DNA a clear footprint can be seen at the target site which persists to an oligonucleotide concentration of 0.3 μM. A clear footprint is still evident when this fragment is complexed with nucleosome core particles, which requires an oligonucleotide concentration of 1−3 μM. However the footprint on core-bound DNA is smaller than that on free DNA and, in contrast to free DNA, bands at the top of the target site (107 and 108) are not protected. This nucleosome-footprint extends over the entire target site on addition of the triplex-binding ligand (not shown). It appears that the nucleosome core attenuates but does not prevent triplex formation at this target site.

TyrT(107−120). In this final sequence the oligopurine target site was moved along the original *tyr*T sequence to between bases 107 and 120. This sequence contains a 14 base pair oligopurine tract (GAGAAGGGAGAAGG) which can be targeted with the parallel triplex forming oligonucleotide CTCTTCCCTCTTCC generating 6×T·AT and 8×C^+·GC triplets and the antiparallel oligonucleotide GGTTGTGGGTTGTG generating 6×T·AT and 8×G·GC triplets. In Figure 8, panels a and b show the results for parallel triplex formation at this target site. Panel a shows DNase I digestion of free DNA for which a clear footprint can be seen at the target site which persists to an oligonucleotide concentration of 0.3 μM. On placing this DNA fragment onto the nucleosome cores, a footprint is still observed with this oligonucleotide which persists to a concentration of 1 μM. Enhanced DNase I cleavage products can also be seen in regions above and below this target site.

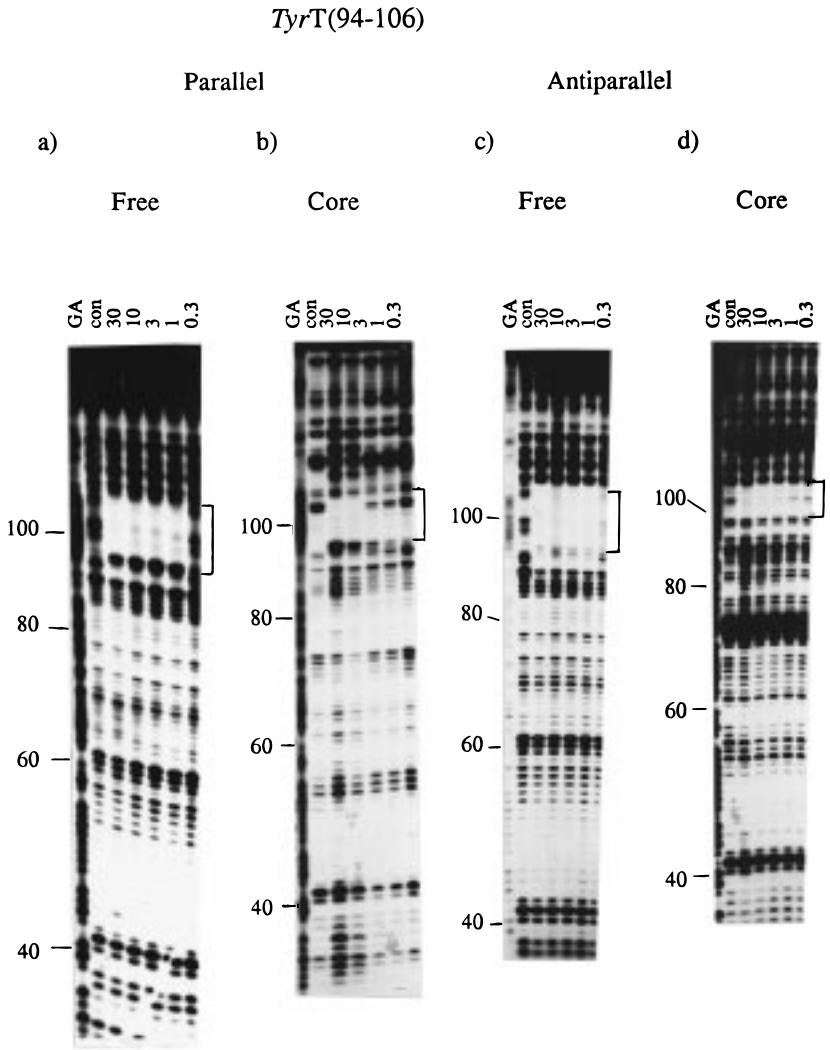

FIGURE 7: DNase I cleavage patterns of *tyr*T(94−106) in the presence and absence of parallel and antiparallel oligonucleotides when free or complexed with nucleosome core particles. The position of the triplex target site is indicated by the square brackets. "con" indicates cleavage of the DNA in the absence of oligonucleotide. Oligonucleotide concentrations (μM) are indicated at the top of each gel lane. Tracks labeled "GA" are Maxam−Gilbert sequencing lanes specific for purines. Panels a and b show the results of parallel triplex formation and were performed in 50 mM sodium acetate pH 5.5 containing 50 mM NaCl and 10 mM $MgCl_2$. Panels c and d show antiparallel triplex formation and were performed in 10 mM Tris-HCl pH 7.5 containing 10 mM $MgCl_2$ and 100 mM NaCl.

The results for antiparallel triplex formation at this site are shown in panels c and d of Figure 8. This G-rich oligonucleotide also produces a clear DNase I footprint without addition of the triplex-binding ligand, which persists to a concentration below 0.3 μM. On wrapping this DNA fragment around the nucleosome cores a footprint can still be seen, although this requires higher oligonucleotide concentrations (10 μM and above). Once again the protein core appears to hinder but not prevent triplex formation. Oligonucleotide-induced enhanced cleavage is again evident in the region above the target site, around position 130. Cleavage of this position is also strong for free DNA, suggesting that the oligonucleotide has caused this DNA section to move away from the protein surface.

DISCUSSION

The results presented in this paper have systematically analyzed how the position of nucleosome bound target sites affects triplex formation. By mutating the *tyr*T sequence we have prepared 7 DNA fragments containing 12−14 base oligopurine tracts at different locations. Hydroxyl radical cleavage of these fragments has shown that six of them adopt the same rotational position on nucleosome core particles as the native *tyr*T DNA. These can therefore be used directly to compare the effect of nucleosome position on triplex formation. The results for the formation of parallel and antiparallel triplexes on free and core-bound DNA are summarized in Table 2. From these data it appears that one of the important factors affecting the formation of triplexes on nucleosome-bound DNA is the location of the target site along the nucleosomal fragment. Oligopurine tracts closer to the center of the DNA fragment, which are presumably closer to the nucleosome dyad, less readily form triplexes. In the Discussion below we will first consider the interaction of the DNA fragments with the nucleosome cores before addressing the formation of antiparallel and parallel triplexes in turn.

Rotational and Translational Positions of the Target Sites. The hydroxyl cleavage patterns presented in Figure 2 suggest that each of the fragments, with the exception of *tyr*T(62−75), adopts the same rotational position with respect to the nucleosome surface. This is not surprising since these

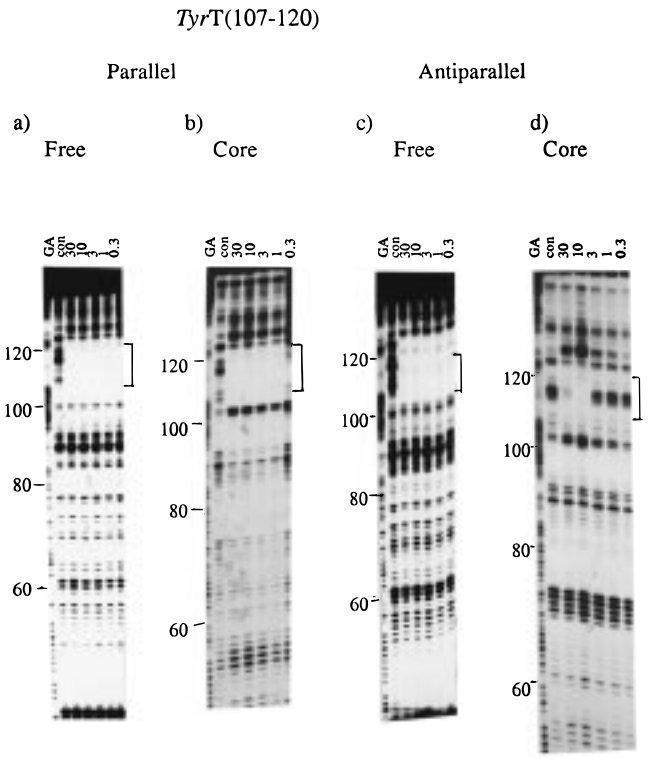

FIGURE 8: DNase I cleavage patterns of *tyr*T(107−120) in the presence and absence of parallel and antiparallel oligonucleotides when free or complexed with nucleosome core particles. The position of the triplex target site is indicated by the square brackets. "con" indicates cleavage of the DNA in the absence of oligonucleotide. Oligonucleotide concentrations (μM) are indicated at the top of each gel lane. Tracks labeled "GA" are Maxam−Gilbert sequencing lanes specific for purines. Panels a and b show the results of parallel triplex formation and were performed in 50 mM sodium acetate pH 5.5 containing 50 mM NaCl and 10 mM $MgCl_2$. Panels c and d show antiparallel triplex formation and were performed in 10 mM Tris-HCl pH 7.5 containing 10 mM $MgCl_2$ and 100 mM NaCl.

Table 2: Lowest Oligonucleotide Concentrations Required To Produce DNase I Footprints on the Various *tyr*T Fragments When Free or Nucleosome Bound

	concentrations,[a] μM			
	parallel		antiparallel	
target	free	core	free	core
*Tyr*T(22−33)	<0.3	1	3	3
*Tyr*T(39−50)	0.3	no	0.3	no
*Tyr*T(43−54)[b]	0.3	no	3	no
*Tyr*T(48−59)	<0.3	30	1	no
*Tyr*T(62−75)	1	1	<0.3	no
*Tyr*T(94−106)	1	10	0.3[†]	1[†]
*Tyr*T(107−120)	<0.3	1	<0.3[†]	10[†]

[a] All experiments with the GT-containing oligonucleotide, generating antiparallel triplexes, contained 10 μM of the naphthylquinoline triplex-binding ligand, except those marked ([†]). No indicates no triplex formation evident at the highest oligonucleotide concentration (30 μM). [b] Data for *tyr*T(43−54) are taken from ref 37.

sequences were prepared so as to cause the smallest changes relative to the original fragment and had at most three base changes. It would therefore be surprising if these minor changes had altered the rotational position of the entire fragment, especially since sequences toward the center of the nucleosome core, closest to the dyad are known to have the greatest effect on rotational position. It should however be remembered that the translational position of these fragment has not been confirmed and we must consider the possibility that in some instances the nucleosome has slipped along the DNA molecule. This is especially relevant since the *tyr*T DNA fragment is 160 base pairs long, while the length of DNA in contact with the protein surface is about 145 base pairs. Previous studies have suggested that in the native fragment positions 0−145 are in contact with the protein (*25*). The nucleosome could therefore move by 10 base pairs in one direction (i.e., covering bases 10−155) and retain both the rotational setting and the total number of protein−DNA contacts. Further translational movement would seem less likely since this would result in fewer contacts between DNA and protein, leaving part of the DNA-binding surface of the nucleosome unoccupied, with one or other end of the DNA fragment hanging free in solution. We have attempted to resolve this question by examining the digestion of these reconstituted DNA fragments with micrococcal nuclease (not shown). However, apart from differences caused by simple changes in the DNA base sequence, these nucleosome-bound fragments showed similar digestion patterns, which were not affected by interaction with the third strand oligonucleotides. A simple interpretation of our data assumes that each of the DNA fragments (except 62−75) adopts the same translational position. However, it is possible that this is not the case, and could be altered upon interaction with the triplex-forming oligonucleotides.

In contrast the patterns observed with *tyr*T(62−75) show evidence for a change in rotational and/or translational setting. Although the hydroxyl radical cleavage patterns for this fragment confirm that it is bound to the protein surface the simple 10 base pair repeat is lost, suggesting that it can adopt at least two energetically equivalent rotational positions. In addition the DNase I patterns suggest that the nucleosome has moved along this DNA fragment so that the first 50 bases are now hanging free in solution. These changes are consistent with the suggestion that sequences around the nucleosome dyad have the greatest effect on nucleosome positioning. If oligopurine tracts are normally excluded from the region of the nucleosome dyad, then this may facilitate triplex formation in vivo, since such target sequences are therefore more likely to be found in regions of nucleosomal DNA which are more accessible for triplex formation.

Although the experiments with CT-containing oligonucleotides were performed in nonphysiological conditions (pH 5.5), necessary for protonation of the third strand cytosines, we find that this did not affect the interaction of the DNA with the nucleosome surface. The rotational position, as evidenced by hydroxyl cleavage remained largely unchanged. Although there are subtle changes between the DNase I cleavage patterns of core-bound DNA at pH 5.5 and 7.5, which are more pronounced than those on free DNA, these do not suggest a change in the DNA location.

Antiparallel Triplexes. The results with antiparallel triplex formation are the easiest to understand since these show a clear correlation between the position of the target site and successful triplex formation. Nucleosome-bound antiparallel triplexes could be formed on *tyr*T(22−33), *tyr*T(94−106) and *tyr*T(107−120), but not on *tyr*T(39−50), *tyr*T(43−54), *tyr*T(48−59) and *tyr*T(62−75). It therefore appears that it

is possible to target approximately the first and last 30−40 bases of nucleosomal DNA with GT-containing oligonucleotides.

It is interesting to note that most of these antiparallel triplexes required the addition of a triplex-binding ligand for successful complex formation, even with free DNA. The observation that this ligand does not disrupt nucleosomes is in itself interesting and confirms that this compound binds to triplex rather than duplex DNA. In addition it should be noted that the footprints are only observed at the intended target sites on the core DNA, even though other studies with free DNA have shown that the ligand causes some loss of stringency with parallel triplexes, promoting triplex formation at related sequences (*46*). The lower stability of antiparallel triplexes may account for the different results seen with parallel and antiparallel triplexes on *tyr*T(48−59) and *tyr*T(62−75). As discussed below the more tightly binding parallel triplexes may be able locally to displace the DNA from the protein surface.

The weak binding of most of these antiparallel triplexes may arise since they consist mainly of T·AT rather than G·GC triplets. It has been previously suggested that the formation of antiparallel triplexes is dominated by the stability of blocks of G·GC triplets, with T·AT and A·AT playing a relatively minor role. This is substantiated by the observation that antiparallel triplexes can be formed on *tyr*T(94−106) and *tyr*T(107−120) without addition of this ligand; these complexes contain a much higher proportion of G·GC triplets. We also attempted to form antiparallel triplexes at *tyr*T(43−54) using GA-containing oligonucleotides, but without success.

We should also consider the possibility that in some instances the third strand oligonucleotide binds to the nucleosomal fragment but does not span the entire target site. In many instances DNase I cleavage of the target site is poor, so that triplex formation is only detected by clear changes in the intensity of a few bands within the target. There is some evidence for this possibility from changes in the extent of the footprints observed with *tyr*T(22−33) and *tyr*T(94−106). Apart from these subtle changes at the edges of the triplex target sites we can generally exclude this possibility, since interaction with only a portion of the target site would produce insufficient triplets to generate a stable complex. Indeed these short triplexes (<14 bases) were designed to exclude this possibility.

Parallel Triplexes. The studies with parallel triplexes show successful complex formation with *tyr*T(22−33), *tyr*T(94−106), *tyr*T(48−59), *tyr*T(62−75) and *tyr*T(107−120) but not with *tyr*T(39−50) and *tyr*T(43−54). Many of these results follow the trend seen with the antiparallel complexes; the exceptions are *tyr*T(48−59) and *tyr*T(62−75) which show parallel but not antiparallel triplex formation. These differences could be caused by several factors including the greater stability of parallel triplexes, the lower pH required for these experiments and their different structures. The inability to form nucleosome-bound triplexes on both *tyr*T(39−50) and *tyr*T(43−54) suggests that the rotational position of the target site alone is not responsible for the lack of triplex formation, since these two targets are separated by half a helical turn.

If we assume that triplex DNA is incompatible with a native nucleosome structure, then triplex formation will depend on a local competition between the oligonucleotide and the protein for the duplex target site. The most stable triplexes will therefore be better able to form nucleosomal complexes; as a result we would expect parallel triplexes to form more readily on nucleosomal DNA than their antiparallel counterparts.

This successful formation of triplexes at regions closest to the ends of the nucleosomes is consistent with the mechanism proposed for the access of proteins to chromatin-bound DNA (*48, 49*). In this model the nucleosomes are dynamic structures in which regions of DNA can become transiently exposed and thereby recognized by DNA-binding agents. DNA sequences closest to the ends of nucleosomal fragments will be exposed more frequently and will therefore show apparently greater binding constants. In addition oligonucleotides which bind the fastest (tightest) will be able to stabilize those nucleosome structures with dissociated or frayed ends. However, this model does not entirely support the results presented in this paper, for it would suggest that successful triplex formation should leave the reminder of the DNA fragment, which has pealed off from the nucleosome surface, hanging free in solution. In this case the DNase I cleavage pattern on the side of the triplex which is closest to the end of the fragment would be expected to resemble free and not core-bound DNA. In some instances there is some evidence for such fraying; for example new bands are evident above the target site with *tyr*T(107−120) in the presence of the oligonucleotide around position 127, and for *tyr*T(94−106) for which several new oligonucleotide-induced cleavage products are evident above the target site (Figure 7b). However, there is little evidence for long range dissociation of DNA from the protein surface. Its rather appears that these short triplexes cause the DNA to move away from the protein surface, only in the vicinity of their binding sites.

Since the hydroxyl radical experiments suggest that *tyr*T(62−75) is not located in the same orientation(s) as the other fragments, the results with this fragment can be explained by suggesting that the target site is actually located much closer to the end of the nucleosomal DNA than otherwise predicted. Since this nucleosome-bound sequence forms complexes with parallel but not antiparallel triplexes it seems reasonable to suppose that the target site is located in a position intermediate between that in *tyr*T(22−33), which forms both parallel and antiparallel triplexes, and *tyr*T(*39*−*54*) which forms neither complex.

The results with *tyr*T(*48*−*59*) are less easily explained. This target site is one helical turn away from that in *tyr*T(*39*−*50*) for which triplex formation was not possible. The differences cannot therefore be attributed to variations in the rotational position of the target sites. Arguments which suggest that this fragment adopts a different translational position might explain the anomalous results with parallel triplexes. However the observation that antiparallel triplexes cannot be formed on this fragment confirm that this target site is located within the DNA region which is in contact with the protein. Although the parallel triplex is readily formed on free DNA the affinity of this oligonucleotide for core-bound DNA is reduced by about 100-fold (footprinting at 30 μM in contrast to 0.3 μM) and has the lowest affinity of all the successful core-bound parallel triplexes. We suggest that although this oligopurine tract is wrapped around the protein core and adopts a similar rotational setting to

the target site in *tyr*T(39−50), this extended oligopurine tract is occluded from interaction with the oligonucleotide and is forced to adopt an unfavorable configuration. As a result it can be prised away from the protein surface by the triplex forming oligonucleotide. This may explain the altered cleavage seen below the target site *tyr*T(48−59) in Figure 5b.

Conclusions. The results presented in this paper show that in some instances intermolecular DNA triple helixes can be successfully formed on fragments which have been complexed with nucleosome core particles. This is in contrast to our previous observations (*37*) and other studies which have attempted to reconstitute DNA fragments after triplex formation (*36*). Although it seems reasonable to expect nucleosomes to exclude regions of triplex DNA on account of its structure, charge or rigidity, the observed biological effects of triplex formation in vivo suggest that there must be some interaction with chromatin-bound target sequences. We can envisage several ways in which this might be possible. First, as suggested by the results presented in this paper, triplexes may form on regions of DNA which are less tightly associated with the protein surface, typically those DNA regions which are located toward the ends of each nucleosome. We have recently demonstrated a similar effect for $A_n \cdot T_n$ tracts which are also less readily incorporated into nucleosomes (*50*). Triplexes can be formed on these tracts in nucleosome-bound fragments in which the DNA remains bound to the nucleosome surface but is moved away from the protein surface in the vicinity of the triplex. Second the formation of the triplex may cause some nucleosome remodeling, causing a change in the translational position of the DNA. We cannot exclude this possibility for some of the results presented in this paper, and this may be a reasonable explanation for the formation of parallel triplex with *tyr*T(48−50). However, this cannot be a general phenomenon since we have demonstrated several instances where triplex formation is prevented by nucleosome formation. A third possibility is that triplex formation in vivo might be facilitated by transcription, when DNA is less firmly attached to the protein surface.

In general the results presented in this paper demonstrate that triplex formation is only possible on the first 40 or so base pairs from the ends of nucleosome-bound DNA. It therefore appears that 50% of the nucleosome-bound DNA in eukaryotic cells will not be available for targeting by triplex-forming oligonucleotides. However, several other factors should also be considered. First, the present studies have not included either linker DNA or histone H1. Histone H1 may anchor the nucleosomal ends and reduce their dynamic movement preventing these DNA regions from becoming transiently exposed. However this may not be a problem for the practical use of triplex-forming oligonucleotides as antigene agents as histone H1 is often absent from actively transcribed genes (*51*, *52*). A second consideration is that oligopurine triplex target sites are less likely to be found around the nucleosome dyad, and their distribution will be biased toward the more accessible regions of nucleosomal DNA. Third for the therapeutic use of oligonucleotides as antigene agents it will only be necessary to target active genes, which will be less tightly associated with nucleosome structures and more readily accessed for triplex formation. It should also be remembered that the present studies have examined the interaction of triplex forming oligonucleotides with DNA fragments, which have already been complexed with nucleosomes. In contrast other studies have shown that prior triplex formation on longer fragments causes a change in nucleosome phasing on reconstitution so that the triplexes are selective located in the regions of internucleosomal DNA (*35*, *36*).

REFERENCES

1. Sinden, R. R. (1994) *DNA Structure and Function*, Acadmic Press, New York.
2. Soyfer, V. N., and Potaman, V. N. (1996) *Triple-helical Nucleic Acids*, Springer-Verlag, New York.
3. Wells, R. D., Collier, D. A., Hanvey, J. C. Shimizu, M., and Wohlrab, F. (1988) *FASEB J. 2*, 2939−2949.
4. Frank-Kamenetskii, M. D., and Mirkin, S. M. (1995) *Annu. Rev. Biochem. 64*, 65−95.
5. Moser, H. E., and Dervan, P. B. (1987) *Science 238*, 645−650.
6. Sun, J.-S. and Hélène, C. (1993) *Curr. Opin. Struct. Biol. 3*, 345−356.
7. Thuong, N. T., and Hélène, C. (1993) *Angew. Chem. 32*, 666−690.
8. Amirhaeri, S., Wohlrab, F., and Wells, R. D. (1995) *J. Biol. Chem. 270*, 3313−3319.
9. Brahmachari, S. K., Sarkar, P. S., Raghavan, S., Narayan, M., and Matai, M. K. (1997) *Gene 190*, 17−26.
10. Hélène, C. (1991) *Anticancer Drug Des. 6*, 569−584.
11. Hélène, C. (1993) *Curr. Opin. Biotechnol. 4*, 29−36.
12. Chubb, J. M., and Hogan, M. E. (1992) *Trends Biotechnol. 10*, 132−136.
13. Chan, P. P., and Glazer, P. M. (1997) *J. Mol. Med. 75*, 267−282.
14. Lee, J. S., Wordsworth, M. L., Latimer, L. J. P., and Morgan, A. R. (1984) *Nucleic Acids. Res. 12*, 6603−6614.
15. Xodo, L. E., Manzini, G., Quadrifoglio, F., van der Marel, G., and van Boom, J. (1991) *Nucleic Acids Res. 19*, 5625−5631.
16. Beal, P. A., and Dervan, P. B. (1991) *Science 251*, 1360−1363.
17. Radhakrishnan, I., and Patel, D. J. (1993) *Structure 1*, 135−152.
18. Radhakrishnan, I., de los Santos, C., and Patel, D. J. (1993) *J. Mol. Biol. 234*, 188−197.
19. Finch, J. T., Lutter, L. C., Rhodes, D., Brown, R. S., Rushton, B., Levitt, M., and Klug, A. (1977) *Nature 269*, 29−36.
20. Richmond, T. J., Finch, J. T., Rushton, B., Rhodes, D., and Klug, A. (1984) *Nature 311*, 532−537.
21. Burlingame, R. W., Love, W. E., Wang, B.-C., Hamlin, R., Xuong, N.-H. and Moudrianakis, E. N. (1985) *Science 228*, 546−553.
22. Luger, K., Mäder, A. W., Richmond, R. K., Sargent, D. F., and Richmond, T. J. (1997) *Nature 389*, 251−260.
23. Ramsay, N. (1986) *J. Mol. Biol. 189*, 179−188.
24. Drew, H. R., and Calladine, C. R. (1987) *J. Mol. Biol. 195*, 143−173.
25. Drew, H. R., and Travers, A. A. (1985) *J. Mol. Biol. 186*, 773−790.
26. Pennings, S., Muyldermans, S., Meersseman, G., and Wyns, L. (1989) *J. Mol. Biol. 207*, 183−192.
27. Hayes, J. J., Tullius, T. D., and Wolffe, A. P. (1990) *Proc. Natl. Acad. Sci. U.S.A. 87*, 7405−7409.
28. Travers, A. A. (1989) *Annu. Rev. Biochem. 58*, 427−452.
29. Kunkel, G. R., and Martinson, H. G. (1981) *Nucleic Acids Res. 9*, 6859−6888.
30. Puhl, H. L., Gudibande, S. R., and Behe, M. J. (1991) *J. Mol. Biol. 222*, 1149−1160.
31. Fox, K. R. (1992) *Nucleic Acids Res. 20*, 1235−1242.
32. Schrader, T. E., and Crothers, D. M. (1989) *Proc. Natl. Acad. Sci. U.S.A. 86*, 7418−7422.
33. Hayes, J. J., Clark, D. J., and Wolffe. A. P. (1991) *Proc. Natl. Acad. Sci. U.S.A. 88*, 6829−6833.

34. Hayes, J. J., Bashkin, J., Tullius, T. D., and Wolffe, A. P. (1991) *Biochemistry 30*, 8434−8440.
35. Espinás, M. L., Jimenez-Garcia, E., Martinez-Balbas, A., and Azorin, F. (1996) *J. Biol. Chem. 271*, 31807−31812.
36. Westin, L., Blomquist, P., Milligan, J. F., and Wrange, Ö. (1995) *Nucleic Acids Res. 23*, 2184−2191.
37. Brown, P. M., and Fox, K. R. (1996) *Biochem. J. 319*, 607−611.
38. Wilson, W. D., Tanious, F. A., Mizan, S., Yao, S., Kiselyov, A. S., Zon, G., and Strekowski, L. (1993) *Biochemistry 32*, 10614−10621.
39. Cassidy, S. A., Strekowski, L., Wilson, W. D., and Fox, K. R. (1994) *Biochemistry 33*, 15338−15347.
40. Chandler, S. P., Strekowski, L., Wilson, W. D., and Fox, K. R. (1995) *Biochemistry 34*, 7234−7242.
41. Satchwell, S. C., Drew, H. R., and Travers, A. A. (1986) *J. Mol. Biol. 191*, 659−675.
42. Wall, G., Varga-Weisz, P. D., Sandatzopoulos, R., and Becker, P. B. (1995) *EMBO J. 14*, 1727−1736.
43. Tsukiyama, T., Becker, P. B., and Wu, C. (1994) *Nature 367*, 525−532.
44. Drew, H. R., and Travers, A. A. (1984) *Cell 37*, 491−502.
45. Travers, A. A., Lamond, A. I., Mace, H. A. F., and Berman, M. L. (1983) *Cell 35*, 265−273.
46. Brown, P. M., Drabble, A., and Fox, K. R. (1996) *Biochem. J. 314*, 427−432.
47. Keppler, M. D., and Fox, K. R. (1997) *Nucleic Acids Res. 25*, 4464−4469.
48. Polach, K. J., and Widom. J. (1995) *J. Mol. Biol. 254*, 130−149.
49. Polach, K. J., and Widom, J. (1996) *J. Mol. Biol. 258*, 800−812.
50. Brown, P. M., and Fox, K. R. (1998) *Biochem. J. 333*, 259−267.
51. Felsenfeld, G. (1992) *Nature 355*, 219−224.
52. Wolffe, A. P. (1994) *Curr. Opin. Genet. Dev. 4*, 245−254.

BI981768N